Article published online: 2024-04-21

Original Article

Can Dynamic Contrast-Enhanced MRI be Used to Differentiate Hepatic Hemangioma from Other Lesions in Early Infancy?

Dan Halevy[1,2] Blayne A. Sayed[3,4] Furqan Shaikh[5,6] Iram Siddiqui[6,7] Govind B. Chavhan[1,2]

[1] Department of Diagnostic Imaging, The Hospital for Sick Children, Toronto, Ontario, Canada
[2] Department of Medical Imaging, University of Toronto, Toronto, Ontario, Canada
[3] Division of General and Thoracic Surgery, The Hospital for Sick Children, Toronto, Ontario, Canada
[4] Department of Surgery, University of Toronto, Toronto, Ontario, Canada
[5] Division of Hematology and Oncology, The Hospital for Sick Children, Toronto, Ontario, Canada
[6] Department of Pediatrics, University of Toronto, Toronto, Ontario, Canada
[7] Department of Pediatric Laboratory Medicine, The Hospital for Sick Children, Toronto, Ontario, Canada

Address for correspondence Govind B. Chavhan, MD, DABR, Department of Diagnostic Imaging, The Hospital for Sick Children, 555 University Avenue, Toronto, ON M5G 1X8, Canada (e-mail: drgovindchavhan@yahoo.com).

Indian J Radiol Imaging

Abstract

Background Confident diagnosis of hepatic hemangioma on imaging can avoid biopsy in early infancy and helps guide conservative management.

Purpose This article aims to determine if dynamic contrast-enhanced magnetic resonance imaging (MRI) can be used to differentiate liver hemangioma from other lesions in infants $\leq$ 100 days and to determine association of MRI features with hepatic lesions.

Methods MRI performed for liver lesions were retrospectively reviewed to note imaging characteristics and the MRI diagnosis. Final diagnosis was assigned based on pathology in available cases and by corroborative standard of reference including overall clinical features, lab findings, and follow-up.

Results Of 30 infants (18 boys, 12 girls; average age 42.2 days) included, 18 had solitary and 12 had multifocal lesions. Diagnoses in total 33 lesions included hemangiomas (23), hepatoblastoma (6), arteriovenous malformation (2), neuroblastoma metastases (1), and infarction (1). MRI and final diagnosis matched in 94% lesions with almost perfect agreement (kappa 0.86) for reader 1, and matched in 88% lesions with substantial agreement (kappa 0.71) for reader 2. Interobserver agreement for MRI diagnosis was substantial (kappa 0.62). Sensitivity, specificity, positive predictive value, negative predictive value, and accuracy of MRI in differentiating hemangioma from other lesions were 100, 90, 96, 100, and 97%, respectively. Centripetal (16/23) or flash (5/23) filling were only seen with hemangioma. There was no significant

Keywords
- liver
- neonate
- infants
- hemangioma
- hepatoblastoma
- imaging

DOI https://doi.org/10.1055/s-0044-1785208.
ISSN 0971-3026.

Thieme Medical and Scientific Publishers Pvt. Ltd., A-12, 2nd Floor, Sector 2, Noida-201301 UP, India

difference in alpha-fetoprotein elevation (p 0.08), average size (p 0.35), multifocality (p 0.38), and intralesional hemorrhage (p 1) between hemangioma and hepatoblastoma. **Conclusion** Centripetal filling on dynamic imaging and absence of washout are characteristic MRI features of hepatic hemangioma that can help to differentiate it from other lesions in early infancy.

Introduction

Hepatic tumors account for only 4% of all neonatal tumors but can be associated with significant morbidity and mortality.[1] Hepatic hemangioma is the most common neonatal hepatic tumor accounting for > 60% cases.[2] This is followed by hepatoblastoma and mesenchymal hamartoma. Nonneoplastic liver lesion may be seen occasionally in infants including liver abscesses and line-related hematomas.

Hepatic hemangioma is a benign proliferative endothelial cell neoplasm that shows characteristic phases of rapid growth caused by cellular proliferation and spontaneous involution.[3] Hepatic hemangiomas can be focal, multifocal, or diffuse. Multifocal and diffuse hemangiomas are usually infantile while most congenital hemangiomas are unifocal.[4,5] Hemangiomas can be completely asymptomatic or can be associated with congestive heart failure, fulminant hepatic failure, rupture and bleeding, hypothyroidism, and abdominal compartment syndrome. Infantile hemangiomas appear after birth and are Glut-1 positive. Congenital hemangiomas are present and thought to be fully grown at birth and are Glut-1 negative.[4] However, recent studies have shown that about a third of congenital hemangiomas can grow after birth before their involution.[6] Regardless of the type, hemangiomas tend to show consistent imaging pattern consisting of T2-hyperintensity and peripheral nodular enhancement on arterial phase images followed by centripetal filling.[4] For the purpose of this study, a collective term "hepatic hemangioma" is used to include both infantile and congenital hemangiomas. It is also worthwhile to note that the term "hemangioendothelioma" should not be used for infantile or congenital hemangioma and it should be reserved for more aggressive lesions such as epithelioid hemangioendothelioma and kaposiform hemangioendothelioma. Note should also be made that hepatic "hemangiomas" seen in adult livers are not true hemangiomas but venous malformations.

Hepatoblastoma is the most common primary malignant tumor in pediatric liver with median age of presentation around 2 years.[7] However, they can present in neonatal age group and often are in the differentials diagnosis for a neonate with a liver tumor. Hepatoblastoma is usually large, multilobulated, heterogeneous enhancing lesion with overall lesion remaining hypointense in all phases postcontrast.[8] However, a small lesion or individual focal areas in a large malignant tumors such as hepatoblastoma or hepatocellular carcinoma (HCC) can show arterial phase hyperenhancement (APHE) and washout, which is characteristic feature of a malignant lesion.[9,10] Due to the fact that hemangioma and hepatoblastoma have very different management and prognosis, it is crucial to differentiate them. Other less common liver tumor seen in neonatal age group, mesenchymal hamartoma, is characterized by predominantly cystic appearance.[8]

Role of magnetic resonance imaging (MRI) in characterization and diagnosis of hepatic tumors in adults is well documented and malignant tumors such as HCC can be diagnosed without pathologic confirmation in high risk-patients using Liver Imaging Reporting and Data System criteria.[11] Role of MRI in detection, characterization, and assessment of staging and extent in hepatic lesions is also well described in children.[12,13] However, there is no data on role of MRI in the assessment of hepatic lesions in early infancy. Confident diagnosis of hepatic hemangioma on imaging can avoid biopsy in infants and helps guide conservative management.

The purpose of this study was to determine if dynamic contrast-enhanced MRI can be used to differentiate hepatic hemangiomas from other lesions in infants ≤ 100 days and to determine frequency and association of MRI features with common neonatal hepatic lesions.

Materials and Methods

Institutional Research Ethics Board approval and waiver for individual patient consent was granted for this retrospective study.

Patients

The institutional picture archiving communication system (PACS, GE Healthcare, Milwaukee, Wisconsin, United States) was searched for MRI performed in infants ≤ 100 days of age for known or suspected liver lesions between January 1, 2008 and December 31, 2020. We chose 100 days as cutoff age arbitrarily as most of the hepatic hemangiomas present in this age group. Infants with MRI study that was nondiagnostic, incomplete, or without intravenous contrast were excluded. Only pretreatment imaging was included in this study.

Imaging Technique

Over the study period, MRI was completed on either a 1.5-tesla (T) Avanto (Siemens Healthcare, Erlangen, Germany) or a 1.5-T or 3-T Achieva (Philips Healthcare, Best, The Netherlands). Apart from T1-weighted, T2-weighted, and postcontrast T1-weighted gradient echo images, dynamic postcontrast images in arterial (18–20 seconds), portal venous (55–60 seconds), and equilibrium (3 minutes) phases

and in delayed (> 5 minutes) phases after injection of a standard dose (0.1 mmol/kg) of extracellular gadolinium-based contrast media gadobutrol (Gadovist, Bayer Healthcare, Berlin, Germany) or Magnevist (Gadopentetate, Bayer Healthcare, Berlin, Germany) were acquired (entire protocol in ►**Table 1**). MRI scan was performed using either feed-and-sleep technique, or under sedation provided by the neonatal intensive care unit (NICU) team or under general anesthesia. All sequences acquired were with free breathing.

Imaging Analysis

MRI images were retrospectively reviewed by a pediatric radiologist and a pediatric radiology fellow (13 and 1 years of experience in reading pediatric body MRI, respectively) independently. Both radiologists were blinded to clinical details and laboratory and histology findings.

On MRI, background liver, signal characteristics of lesions on T1-weighted, T2-weighted, in-phase and out-of-phase, arterial phase, portal venous phase, and equilibrium phase images were noted. The dominant signal intensity of the lesion on T1-weighted, fat-suppressed T2-weighted, and fat-suppressed postcontrast T1-weighted images was categorized into four different grades[8]: grade I = hypointense to liver parenchyma, grade II = isointense to liver parenchyma, grade III = slightly hyperintense to liver parenchyma, and grade IV = markedly hyperintense to parenchyma (reaching signal intensity of subcutaneous fat on precontrast T1-weighted images, similar to the intensity of cerebrospinal fluid on T2-weighted images, and similar to intensity of the vessels on postcontrast T1-weighted images). Any specific features such as APHE, washout of entire lesion or part of it in equilibrium and/or portal venous phases, centripetal filling (peripheral nodular enhancement on arterial phase followed by progressive enhancement from periphery to center on later phases), flash filling (homogeneous complete avid enhancement of a lesion in arterial phase), and heterogeneous enhancement (random areas of variable enhancement throughout the tumor without a specific pattern on all phases but mostly on arterial phase) were noted. Presence of exophytic lesion and hemorrhagic products (hyperintense areas within tumor on precontrast T1-weighted fat-saturated images) were also noted. The maximum dimension of tumor was measured in three planes to obtain average diameter. In cases with multiple lesions of same imaging characteristics, the largest lesion was included. In cases with multiple lesions having different imaging features, the largest lesion representing each different imaging features/diagnosis was included.

Both readers also assigned an imaging diagnosis to the lesion based on MRI features. Imaging features for the diagnosis of hemangiomas included marked T2 hyperintensity (grade IV) and centripetal or flash filling without any washout. Imaging features for hepatoblastoma included heterogeneous enhancement, washout, and lack of centripetal filling. Arteriovenous malformation (AVM) showed characteristic features including hypertrophied arteries, early draining veins, and large network of vessels. During the consensus review after independent review by each reader, one best possible imaging diagnosis was assigned to each lesion that was used for analysis. Discrepancies in the imaging features were also resolved in consensus review.

Table 1 Liver MRI protocol

Seq #	Sequence	Plane	TR/TE (ms)	Flip angle (degrees)	Matrix/SL	NSA	ETL	Pixel bandwidth (Hz)	Approximate Time
1	STIR	Coronal	2100/54	150	300 × 196/3 mm	4	9	260	3 min
2	T2 FSE fatsat	Axial	3900/100	160	320 × 240/3 mm	2	19	195	3 min
3	Balanced SSFP	Axial	5/2.5	70	256 × 208/3 mm	4	1	490	3 min
4	T1W in and out phase	Axial	178/4.6 and 2.3 ms	75	256 × 134/3 mm	4	2	415	40 s
5	Pre-Ax VIBE/THRIVE	Axial	3.96/1.62	9	320 × 200/3 mm	3	1	446	20 s
Dynamic IV contrast injection									
6	Ax VIBE/THRIVE (2 NSA) FB dynamic 4 runs	Axial	3.96/1.62	9	320 × 200/3 mm	3	1	446	20 s
7	Ax T1 TSE FS (6 NSA) FB	Axial	648/9.7	130	256 × 200	6	9	332	4 min
8	Ax VIBE/THRIVE (2 NSA) FB delayed at 5–6 min	Axial	3.96/1.62	9	320 × 200/3 mm	3	1	446	20 s

Abbreviations: ETL, echo train length; fatsat, fat-saturated; FB, free breathing; FSE, fast spin-echo; GRE, gradient echo; IV, intravenous; MRI, magnetic resonance imaging; NSA, number of signal averages; SL, slice thickness; SSFP, steady-state free induction (TruFISP/bTFE); STIR, short tau inversion recovery; TE, time to echo; TR, repetition time.

Chart Review and Standard of Reference

Patient charts were reviewed to collect clinical information including alpha-fetoprotein (AFP) levels (normal, elevated by our laboratory age-based reference ranges, and elevated in millions), biopsy results, and imaging follow-up. Pathology was standard of reference in available cases. In cases without pathology, corroborative findings including clinical, laboratory, and imaging features and follow-up of at least 6 months documenting regression or stability of the lesion served as standard of reference for the final diagnosis of lesion.

Statistical Analysis

Baseline and demographic characteristics were summarized using descriptive statistics (means, standard deviations). Interobserver agreement was assessed using kappa test for categorical variables. Kappa values of < 0.20 were considered poor agreement, 0.21 to 0.40 fair agreement, 0.41 to 0.60 moderate agreement, 0.61 to 0.80 substantial agreement, and > 0.80 almost perfect agreement.[14] Sensitivity, specificity, positive predictive value (PPV), negative predictive value (NPV), and accuracy of MRI in diagnosis of hepatic lesion were determined against the reference standard. MRI diagnosis assigned to each case during consensus review was used for this assessment. Fisher's exact test was used to determine association of imaging features with diagnoses. A p-value of < 0.05 was considered significant.

Results

Patients

A total of 103 infants $\leq$ 100 days underwent liver MRI in the study period. After applying inclusion and exclusion criteria (►**Fig. 1**), a total 30 infants (18 boys, 12 girls; median age 42.2 days; range 1–100 days) were included in the final analysis. Sixteen of 30 infants underwent MRI under general anesthesia, 8/30 under sedation provided by the NICU team, and remaining 6/30 with feed-and-sleep technique. Background liver was normal on imaging in 27/30 infants and in the remaining 3/30, there was some degree of siderosis seen as hypointensity of liver parenchyma on in-phase images as compared to out-of-phase images. AFP levels were normal in 16/30 children, elevated but $<$ 1,000,000 ng/L in 11/30, and $>$ 1,000,000 ng/L in 3/30 infants. Time interval between the MRI study and the AFP levels ranged 0 to 120 days with median of 18 days.

Lesions

Of 30 infants, 18 had solitary and 12 had multifocal lesions. Of 33 final diagnoses in total, 8 were assigned by pathology (all 6 hepatoblastomas, 1 hemangioma, and 1 neuroblastoma metastases [primary lesion] were confirmed by histopathology) and 25 by corroborative reference standard with median follow-up period of 29 months (range 6–96 months). Final lesion diagnoses included hemangiomas (23), hepatoblastoma (6), AVM (2), and one each of metastases from neuroblastoma and infarction. The mean average diameter of largest lesions for the entire group was 3.2 cm (range 0.6–10.9 cm).

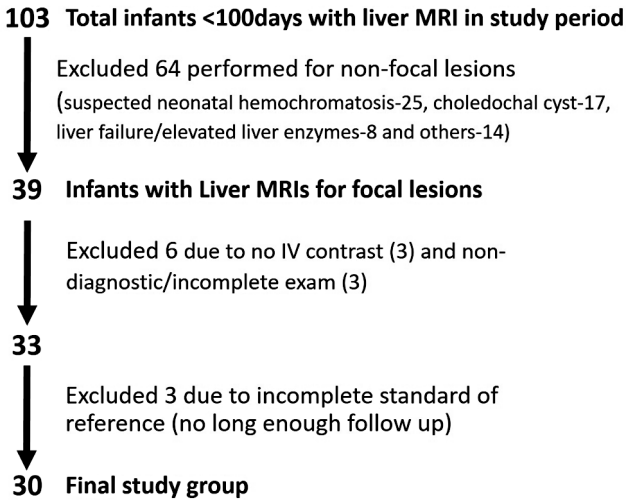

Fig. 1 Flowchart demonstrating patient selection applying inclusion and exclusion criteria.

Hemangiomas: Of 23 hemangiomas (mean average diameter 2.8 cm; range 0.6–7.5 cm) in 23 infants, 16 (70%) were solitary (►**Fig. 2**) and 7 (30%) were multifocal (►**Fig. 3**). Of 16 infants with solitary hemangiomas on imaging, one had associated hepatoblastoma and another had AVM. Twenty-one lesions showed APHE with 16 (76%) showing centripetal filling and 5 (24%) showing flash filling. Thirteen of 16 solitary lesions showed centripetal filling while flash filling was seen in smaller solitary or multifocal lesions, all of which were $<$ 1.5 cm in diameter. None of the 23 hemangiomas showed washout. Six of 23 (26%) lesions were exophytic. AFP levels were normal in 14 of 21 (66%) infants with hemangiomas, elevated in 6/21, and elevated in millions in 1/21 infant who also had a large AVM.

Hepatoblastoma: Of 6 hepatoblastomas (mean average diameter 3.5 cm; range 0.7–10.9 cm) in 5 infants, 3 were solitary (►**Fig. 4**) and 2 were multifocal. In one infant with multiple hepatoblastoma, one of the predominantly cystic lesions was interpreted as mesenchymal hamartoma by both readers, hence 2 hepatoblastomas from this patient were included in the analysis. The smallest lesion in this infant was 0.7 cm in diameter and increased to 3.4 cm on follow-up. APHE was seen in 3 with washout in 1. Four of 6 lesions showed heterogeneous enhancement throughout the lesion and remaining 2 showed predominantly peripheral enhancement. Two lesions were exophytic. AFP levels were normal in one infant, elevated in three, and elevated in millions in two infants.

Interobserver agreement for major MRI features is listed in ►**Table 2**.

Differentiation of Hemangioma from Other Lesions

MRI diagnosis and the final diagnosis matched in 94% lesions with almost perfect agreement (kappa 0.86; 95% confidence interval [CI]: 0.69–1) for reader 1, and matched in 88% lesions with substantial agreement (kappa 0.71; 95% CI: 0.47–0.96) for reader 2. Reader 1 misdiagnosed an infarction as a hemangioma and a hepatoblastoma as mesenchymal hamartoma due to cystic component. Reader 2 misdiagnosed four

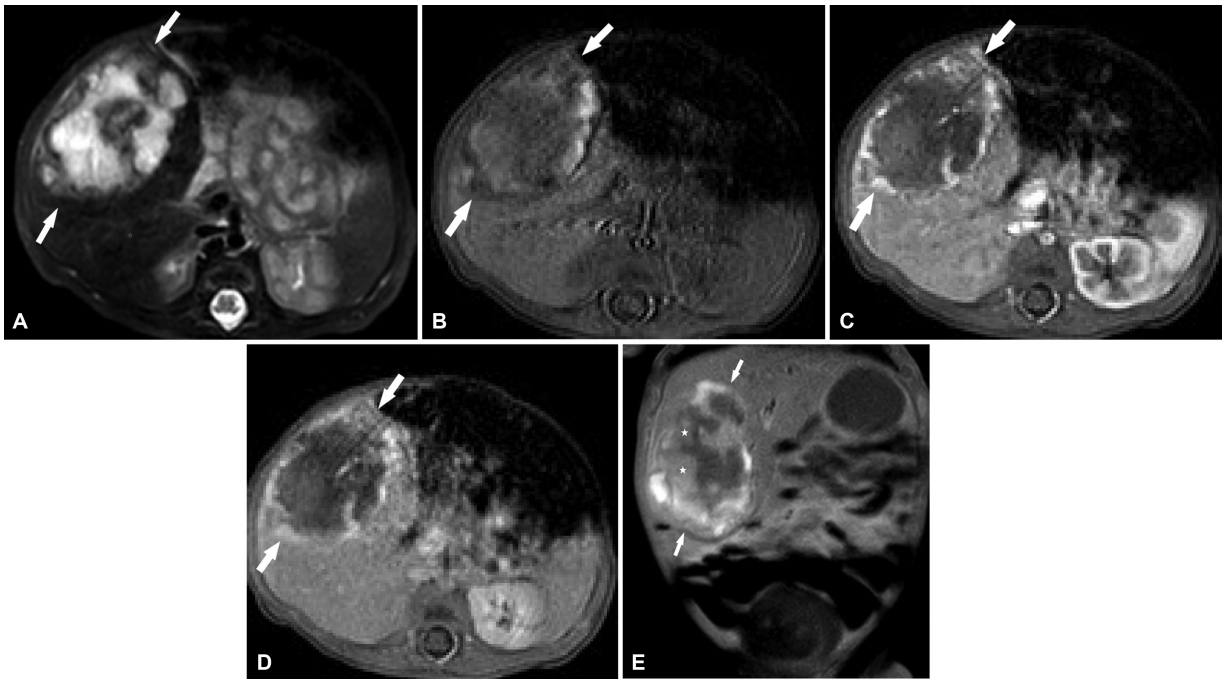

Fig. 2 A large congenital hemangioma in a 6-day-old baby boy. Axial T2-weighted image (**A**) demonstrates a large predominantly hyperintense lesion in the right lobe of liver (arrows). The lesion (arrows) shows some hyperintense areas within it on precontrast axial T1-weighted gradient fat-saturated image (**B**) in keeping with hemorrhage and shows avid peripheral irregular enhancement on postcontrast dynamic images (**C** and **D**). The lesion (arrows) shows some central filling (stars) on delayed postcontrast coronal T1-weighted fat-saturated fast spin-echo image (**E**).

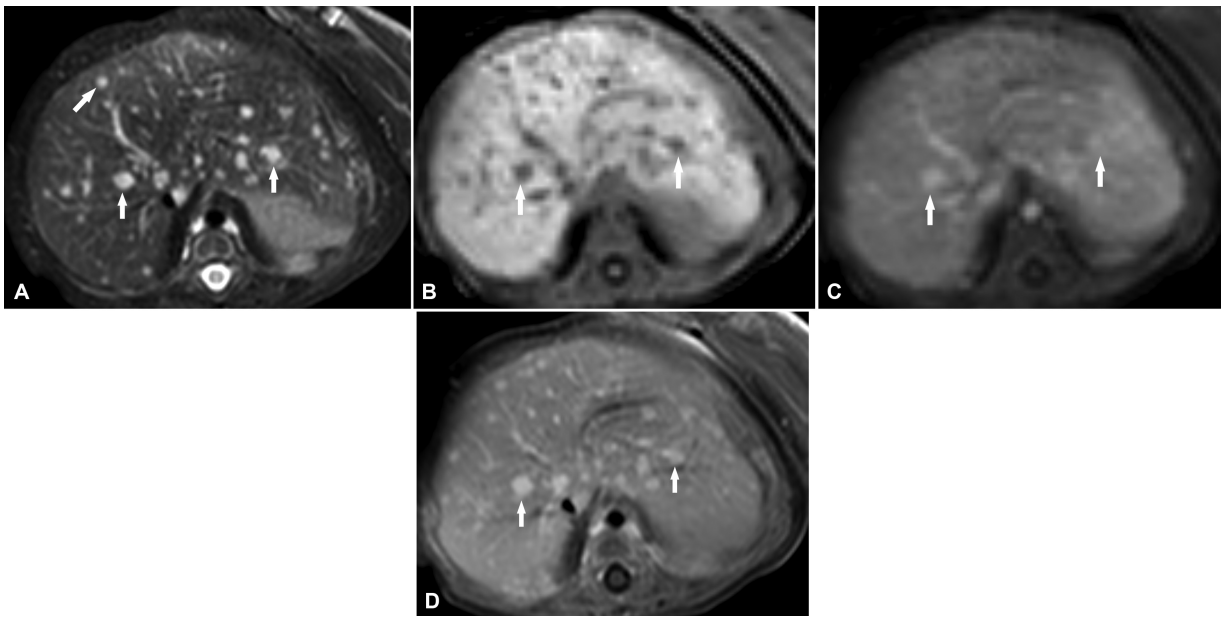

Fig. 3 Multiple small infantile hemangiomas in a 100-day-old baby girl. Axial T2-weighted image (**A**) demonstrates numerous hyperintense lesions (a few marked by arrows) throughout the liver. The lesions (arrows) are hypointense on precontrast axial T1-weighted gradient fat-saturated image (**B**) and show avid complete enhancement on postcontrast T1-weighted gradient fat-saturated dynamic arterial phase (**C**) images in keeping with flash filling. The lesions (arrows) remain hyperintense on delayed postcontrast axial T1-weighted fat-saturated fast spin-echo (**D**) images.

hepatoblastoma, three of which were called as hemangioma and one as metastasis. This discrepancy was resolved with consensus review. The overall interobserver agreement for MRI diagnosis between the two readers was substantial (kappa 0.62; 95% CI: 0.34–0.90). Sensitivity, specificity, PPV, NPV, and accuracy of both readers together in differentiating 23 hemangiomas from other 10 lesions using MRI was 100% (95% CI: 85–100%), 90% (95% CI: 55–100%), 96% (95% CI: 78–99%), 100% (95% CI: 100%), and 97% (95% CI: 84–100%), respectively.

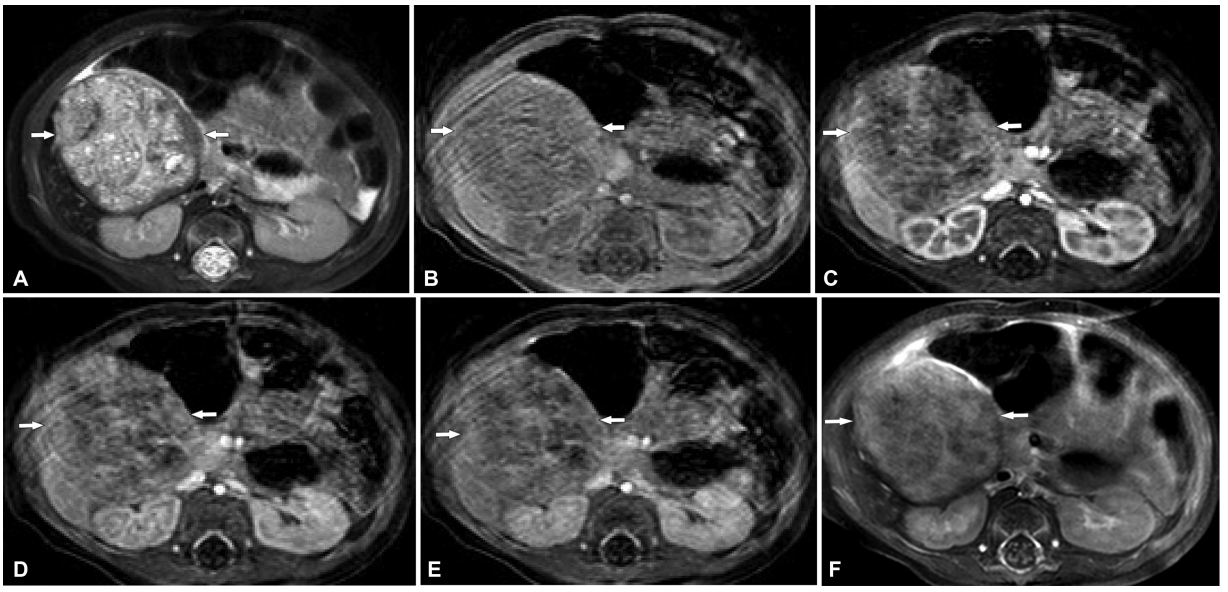

Fig. 4 Hepatoblastoma in a 36-day-old baby boy. Axial T2-weighted image (**A**) demonstrates a large predominantly hyperintense but heterogeneous lesion in the right lobe of liver (arrows). The lesion (arrows) is hypointense on precontrast axial T1-weighted gradient fat-saturated image (**B**) and shows mild heterogeneous enhancement on postcontrast axial T1-weighted dynamic images (**C**–**E**) and remains overall hypointense to normal liver parenchyma. The lesion (arrows) remains heterogeneously enhancing on delayed postcontrast axial T1-weighted fat-saturated fast spin-echo image (**F**).

Table 2 Interobserver agreement between two readers for major MR features

MR feature	Kappa	95% confidence interval
Arterial phase hyperenhancement	0.84	0.53–1.00
Washout	0.21	0.24–0.66
Hemorrhagic product in the lesion	0.74	0.51–0.97
Signal intensity grades on T1-weighted image	1.00	1.00–1.00
Signal intensity grades on T2-weighted image	0.18	0.05–0.41
Imaging diagnosis	0.62	0.34–0.90

Abbreviation: MR, magnetic resonance.

Association of MRI Features with Hepatic Lesions

Centripetal (16/23) or flash (5/23) filling were only seen with hemangioma. There was no significant difference in AFP elevation (p 0.08), average diameter (p 0.35), multifocality (p 0.38), and intralesional hemorrhage (p 1) between hemangioma and hepatoblastoma (►**Table 3**). Washout was seen only with hepatoblastoma (1/6) and metastases (1/1). Heterogeneous enhancement throughout the lesion was only seen with hepatoblastoma (4/6). AVM showed characteristic features including hypertrophied arteries, early draining veins, and large network of vessels (►**Fig. 5**).

Discussion

In this study, we share our experience on utility of dynamic contrast-enhanced MRI for liver lesion assessment in neonatal period and early infancy. Our study demonstrates that a complete dynamic MRI examination with contrast administration can be used for differentiating hemangioma from other hepatic lesions in this age group, in particular, hepatoblastoma. This reliable differentiation can avoid biopsy and guide conservative management for hepatic hemangiomas. One of the disadvantages of MRI, as seen in our study, is need for some form of sedation/anesthesia in majority of infants. However, feed-and-sleep technique, which was mainly used in later part of our study period, also works in majority of infants and is likely to become the main method for MRI scans avoiding proper sedation.

We found that the enhancement pattern is the most important feature that helps to differentiate between the different lesions. More specifically, centripetal filling (in the larger lesions) and flash filling (in the smaller lesions) have very good association with hemangiomas and were not seen with any other lesions (►**Table 1**). These findings were similar to a previous study.[3] Centripetal filling is a characteristic feature of hemangioma and thought to be related to central part occupied by hemorrhage, necrosis, or fibrosis.[15] Flash filling in arterial phase is seen in minority (16%) of adult hemangiomas.[15] In our study, it was seen in 5 lesions, all of which were < 1.5 cm in diameter. These flash-filled hemangiomas retain contrast in

Table 3 Comparison of AFP levels and imaging features in hemangioma and hepatoblastoma

Feature	Hemangioma ($n = 23$)	Hepatoblastoma ($n = 6$)	*p*-Value by Fisher's exact test
AFP level - Normal - Elevated - > 100,000	 14 8 1[a]	 1 3 2	0.08
Multifocal	7	2	0.38
Mean average diameter of largest lesion[b]	3 cm	3.5 cm	0.35
Hemorrhagic products	9	2	1
Centripetal filling	16	0	**0.007**
Flash filling	5	0	0.55
Washout	0	1	0.20
Heterogeneous enhancement	0	4	**0.0006**

Abbreviation: AFP, alpha-fetoprotein.
Note: Flash filling = homogeneous enhancement of the entire lesion in the arterial phase itself, seen usually in smaller lesions < 2 cm.
Bold values indicate statistical significance (<0.05).
[a]This child also had large arteriovenous malformation in the liver.
[b]Average diameter = average of 3 dimensions.

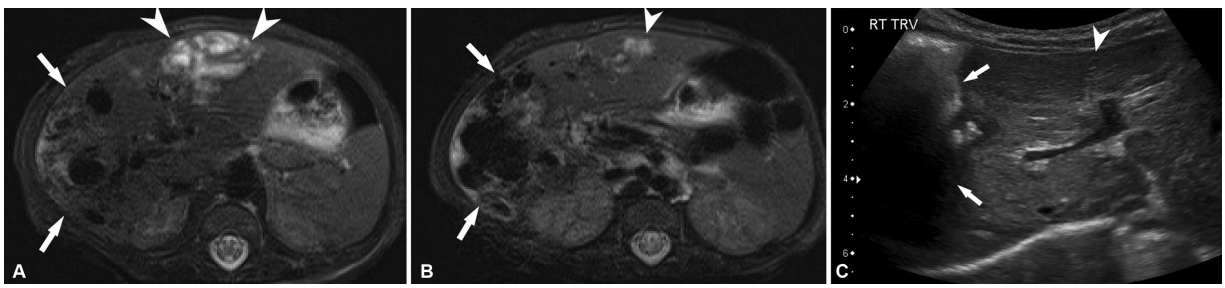

Fig. 5 Arteriovenous malformation (AVM) and hemangioma in an 8-day-old baby boy. Axial T2-weighted images (**A** and **B**) at presentation demonstrate an ill-defined heterogeneous lesion with large vessels (arrows) in the right lobe in keeping with an AVM. In the left lobe, T2 hyperintense lesion (arrowheads) is seen in keeping with hemangioma. On follow-up ultrasound image (**C**) at the age of 11 months, the left lobe lesion (location marked by arrowhead) has resolved and AVM in the right lobe is significantly reduced and mostly obscured by embolization coils (arrows). RT TRV, right transverse image.

delayed phase. Heterogeneous appearance of hepatoblastoma on T1- and T2-weighted as well as on postcontrast images is related to varying amount of necrosis and hemorrhage in the tumor.[16] Heterogeneous enhancement pattern was seen in the majority of the hepatoblastoma lesions in our study and in none of the hemangiomas. Washout on delayed phase was not significantly associated with hepatoblastoma due to small number but none of the 23 hemangiomas showed washout. Washout is typically seen in smaller malignant lesions like hepatoblastoma and HCC.[10] In larger malignant lesions, which is usually the case in children, multiple individual areas need to be assessed that typically show APHE and washout.[10] This possibly explains lower kappa values for washout (k = 0.21) in our study due to less experience of one of the readers. There was no significant difference in association of other imaging feature including lesion size, multifocality, and intralesional hemorrhage between hemangioma and hepatoblastoma.

AFP is a glycoprotein synthesized during fetal life by yolk sac and liver.[17] It is typically elevated in children with malignant tumors such as hepatoblastoma and HCC. However, cautious approach is needed in interpretation in neonatal and early infancy as AFP can be normally elevated in this age group.[17,18] The high AFP levels at birth show exponential reduction with age, typically reaching adult level by end of first year of life. However, there is wide variability in data on reference interval of AFP reduction, limiting its utility in diagnosing these malignant tumors.[17] Also, AFP can be slightly elevated in benign lesions and with hepatic insult and regeneration.[18] In fact, in our study, 6/21 children with hemangiomas showed elevated AFP and another child with both hemangioma and large AVM had AFP levels in millions.

The findings of our study need to be taken in light of several limitations. First, this was a retrospective study. Second, there was a relatively small number of patients with hepatoblastoma (6) and other lesions due to the fact that these lesions are rare in this age group. This limits the ability to determine frequency of their imaging features and reduces statistical power to determine differences between these lesions and hemangiomas. We did not collect any data on clinical presentation of these babies. Lastly, the lack of tissue diagnosis in the cases of suspected hemangioma. Nonetheless, the fact that follow-up imaging showed interval

decrease in the extent of the lesions, increases our confidence in the benign nature of those lesions.

Conclusion

Dynamic contrast-enhanced MRI can be used to differentiate hepatic hemangioma from other lesions in early infancy. Centripetal filling on dynamic imaging, absence of heterogeneous enhancement, and absence of washout are characteristic MRI features of hepatic hemangioma. There was no significant difference in AFP elevation, average diameter, multifocality, and intralesional hemorrhage between hemangioma and hepatoblastoma. When lesion shows heterogeneous enhancement and washout and lack typical centripetal pattern of enhancement, biopsy should be performed. More multicenter studies are needed to validate and strengthen our findings.

Note
This study was presented as an abstract during International Pediatric Radiology Meeting 2021, Rome, Italy.

Funding
None.

Conflict of Interest
None declared.

References

1 Lakhoo K, Sowerbutts H. Neonatal tumours. Pediatr Surg Int 2010; 26(12):1159–1168
2 Isaacs H Jr. Fetal and neonatal hepatic tumors. J Pediatr Surg 2007; 42(11):1797–1803
3 Kassarjian A, Zurakowski D, Dubois J, Paltiel HJ, Fishman SJ, Burrows PE. Infantile hepatic hemangiomas: clinical and imaging findings and their correlation with therapy. Am J Roentgenol 2004;182(03):785–795
4 Iacobas I, Phung TL, Adams DM, et al. Guidance document for hepatic hemangioma (infantile and congenital) evaluation and monitoring. J Pediatr 2018;203:294–300.e2
5 Kulungowski AM, Alomari AI, Chawla A, Christison-Lagay ER, Fishman SJ. Lessons from a liver hemangioma registry: subtype classification. J Pediatr Surg 2012;47(01):165–170
6 Rutten C, Ladarre D, Ackermann O, Gonzales E, Guettier C, Franchi-Abella S. Spontaneous evolution patterns of focal congenital hepatic hemangiomas: a case series of 25 patients. Pediatr Radiol 2022;52(06):1048–1060
7 Darbari A, Sabin KM, Shapiro CN, Schwarz KB. Epidemiology of primary hepatic malignancies in U.S. children. Hepatology 2003; 38(03):560–566
8 Chavhan GB, Shelmerdine S, Jhaveri K, Babyn PS, Liver MR. Liver MR imaging in children: current concepts and technique. Radiographics 2016;36(05):1517–1532
9 Khanna G, Chavhan GB, Schooler GR, et al. Diagnostic performance of LI-RADS version 2018 for evaluation of pediatric hepatocellular carcinoma. Radiology 2021;299(01):190–199
10 Arias GA, Siddiqui I, Navarro OM, Shaikh F, Sayed BA, Chavhan GB. Imaging and clinical features of pediatric hepatocellular carcinoma. Pediatr Radiol 2021;51(08):1339–1347
11 Singal AG, Llovet JM, Yarchoan M, et al. AASLD Practice Guidance on prevention, diagnosis, and treatment of hepatocellular carcinoma. Hepatology 2023;78(06):1922–1965
12 Chavhan GB, Farras Roca L, Coblentz AC. Liver magnetic resonance imaging: how we do it. Pediatr Radiol 2022;52(02):167–176
13 Schooler GR, Squires JH, Alazraki A, et al. Pediatric hepatoblastoma, hepatocellular carcinoma, and other hepatic neoplasms: consensus imaging recommendations from American College of Radiology Pediatric Liver Reporting and Data System (LI-RADS) Working Group. Radiology 2020;296(03): 493–497
14 Viera AJ, Garrett JM. Understanding interobserver agreement: the kappa statistic. Fam Med 2005;37(05):360–363
15 Vilgrain V, Boulos L, Vullierme MP, Denys A, Terris B, Menu Y. Imaging of atypical hemangiomas of the liver with pathologic correlation. Radiographics 2000;20(02):379–397
16 Schooler GR, Hull NC, Lee EY. Hepatobiliary MRI contrast agents: pattern recognition approach to pediatric focal hepatic lesions. AJR Am J Roentgenol 2020;214(05):976–986
17 Ferraro S, Panzeri A, Braga F, Panteghini M. Serum α-fetoprotein in pediatric oncology: not a children's tale. Clin Chem Lab Med 2019; 57(06):783–797
18 Fernandez-Pineda I, Cabello-Laureano R. Differential diagnosis and management of liver tumors in infants. World J Hepatol 2014; 6(07):486–495

